

CHAPTER-IV

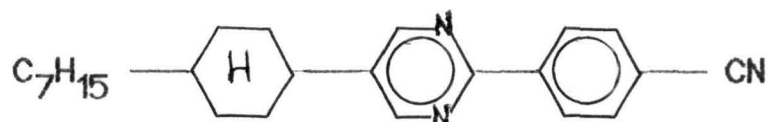
THE CRYSTAL AND MOLECULAR STRUCTURE OF 5-(4-HEPTYLCYCLOHEXYL)-2-

(4-CYANOPHENYL) PYRIMIDINE

4.1 Introduction

The determination of the crystal and molecular structure of the compound 5-(4-heptyl cyclohexyl) -2- (4-cyanophenyl)-pyrimidine (HCCPP) is described in this section. The results of this structural analysis have been published¹. The crystal and molecular structures of the related pentyl and ethyl compounds have already been reported^{2,3}. The knowledge of the conformation and the packing of the mesogenic compounds in the crystalline state gives indication of the conformations and the order in liquid crystalline state leading to a better understanding of the different liquid crystalline phases. Structural studies were undertaken in this context.

The molecular structure of the compound (HCCPP) is given below :



4.2. Diffraction by Crystals

The phenomenon of diffraction by crystals results from a scattering process in which X-rays are scattered by the electrons of the atoms without change in wavelength.

The resulting diffraction pattern comprising of both the positions and the intensities of the diffraction effects, is a fundamental physical property of the substance which is used for the complete elucidation of the structure. To locate the positions of individual atoms in the unit cell, the intensities must be measured and analysed. Most important equation relating the positions of the atoms to the diffraction intensities is given by

$$F_{hkl} = \sum_{j=1}^N f_j \exp 2\pi i (hx_j + ky_j + lz_j) \quad (1)$$

where f_j is the scattering factor or form factor of the j^{th} atom and x_j , y_j and z_j are the fractional coordinates of the j^{th} atom in a unit cell containing N atoms. The observable quantity I is proportional to $|F|^2$.

F_{hkl} can also be expressed in terms of $\rho(xyz)$, the electron density at the point (xyz)

$$F_{hkl} = \int_V \rho(xyz) \exp 2\pi i (hx + ky + lz) dv \quad (2)$$

where V is the volume of the unit cell. Then by Fourier transform we have

$$\rho(xyz) = \frac{1}{V} \sum_h \sum_k \sum_l F_{hkl} \exp -2\pi i (hx+ky+lz) \quad (3)$$

If we could obtain a large number of F_{hkl} by diffraction experiment, we could have directly derive the crystal structure by making a Fourier summation.

Experiments can give the structure amplitudes, $|F_{hkl}|$, but not the phases and this constitutes the phase problem in crystallography. From the intensity data I_{hkl} we determine $|F_{hkl}|$ and direct mathematical relationships are being used to give phase information.

The following sections give the detailed procedure for the structural analysis of the said compound starting from the crystal

data collection.

4.3. Crystal Data Collection

Transparent plate-like crystals were obtained by slow evaporation from a solution of acetone. Lattice parameters and space group were determined by taking oscillation and Weissenberg photographs along different axes. The crystal belongs to monoclinic system. Systematic absences occur for $h0l$ reflections with $l = 2n + 1$ and $0k0$ reflections with $k = 2n + 1$ indicating the space group $P2_1/C$. By floatation technique the density of the crystal was found to be 1.12 gm.cm^{-3} . Taking four molecules per unit cell (i.e. $z = 4$) the calculated density is 1.13 gm.cm^{-3} , close to the observed value.

A crystal of dimension $0.4 \times 0.4 \times 0.3 \text{ mm}^3$ was used for intensity data collection. It was mounted on the tip of a glass fibre and the fibre was in turn fastened to a goniometer head. Accurate cell parameters were determined by a least-squares fit of $\sin\theta$ values of 24 reflections having θ values $45^\circ < \theta < 48^\circ$, measured on an Enraf Nonius CAD-4 diffractometer, using $\text{CuK}\alpha$ radiation monochromatized by a graphite monochromator. A total of 4012 reflections were collected in the $\omega - 2\theta$ scan mode, of which 2951 were above the zero level of $2.5 \sigma(I)$. The data were corrected for Lorentz polarization factors and no absorption correction was necessary. The crystallographic data are given in Table 4.1. The measured value of the intensity is given by

$$I_{\text{raw}} = \frac{A}{n} [C - R.B] \quad (4)$$

where A = attenuation factor (26.55 for $\text{CuK}\alpha$)

n = an integer varying from 8 to 24 to suit the particular

Table 4.1. Summary of crystallographic data

Molecular formula	$C_{24}H_{31}N_3$	
Crystal system	Monoclinic	
Space group	$P2_1/c$	
Form /habit	Plate shaped.	
$a=13.0422(6)$	$b=17.7464(11)$	$c=9.5950(5) \text{ \AA}$
$\beta=107.170(1)^\circ$	$V_c=2121.8094 \text{ \AA}^3$	$D_c=1.13 \text{ gm cm}^{-3}$
$D_o=1.12 \text{ gm cm}^{-3}$	$Z=4$	
Number of independent reflections	4012	
Number of observed reflections	2951	

case.

c = total count.

R = ratio of scan time to background.

B = total background count.

The standard deviation $\sigma(I)$ calculated on the basis of counting statistics is given by

$$\sigma(I_{\text{raw}}) = \frac{20.166}{n} A (C + R^2 B)^{1/2} \quad (5)$$

Applying appropriate Lorentz polarization factor correction⁴⁻⁶ L_p (described below) we get I_{corr} and $\sigma(I_{\text{corr}})$.

$$I_{\text{corr}} = \frac{I_{\text{raw}}}{L_p} \quad \text{and} \quad \sigma(I_{\text{corr}}) = \frac{\sigma(I_{\text{raw}})}{L_p} \quad (6)$$

This intensity value is then converted to $|F_o|$, the observed structure amplitude with

$$|F_o| = K (I_{\text{corr}})^{1/2} \quad (7)$$

K being scalar constant and the corresponding standard deviation is

$$\sigma |F_o| = \frac{\sigma (I_{\text{corr}})}{2 |F_o|} \quad (8)$$

4.4 Intensity Data Reduction

Intensity data collected constitute the raw material from which crystal structures are derived. it is customary to convert the

intensities into observed structure amplitudes by a data reduction program and to use these as the observed data in subsequent calculations.

The relationship between $|F_o|$ and $I^{1/2}$ depends on a number of factors, primarily geometric which relates to the individual reflection and to the apparatus used to measure the intensity. The proportionality can be written as

$$|F_{(hkl)}| = \left(\frac{K I_{hkl}}{L_p} \right)^{1/2} \quad (9)$$

K is called the scale factor, which is normally constant for a given set of measurements and is usually obtained at a later stage.

In our case the incident beam is partially polarized during monochromatization by reflection from the basal plane of a graphite crystal and P takes the form

$$P_{hkl} = P_{erf} \frac{\cos^2 2\theta_m + \cos^2 2\theta_{hkl}}{1 + \cos^2 2\theta_m} + (1 - P_{erf}) \frac{\cos^2 2\theta_m + \cos^2 2\theta_m}{1 + \cos^2 2\theta_m} \quad (10)$$

where P_{erf} = constant depending on the crystal used in the monochromator (= 0.5 in our experiment).

θ_m = Bragg angle of reflection from the monochromator crystal.

The Lorentz factor⁴⁻⁶ L depends on the precise measurement technique used and for diffraction data it is given by

$$L_{hkl} = \frac{1}{\sin^2 \theta_{hkl}} \quad (11)$$

Temperature factor

While introducing the idea of atomic scattering factor f , we have not taken into consideration the finite size of the atom i.e. of the electron cloud about the atomic nucleus and also the thermal vibration of the atom, which increases the effective volume of the electron cloud. Because of the first effect, the scattered intensity falls off with increasing $\sin\theta/\lambda$ and the second factor acts for more rapid fall. The first effect is corrected by taking f values from standard f vs. $\sin\theta/\lambda$ curve^{7,8} and the effect of thermal vibration can be taken care by multiplying f_0 , the form factor for an atom at rest, by a factor⁹ $\exp\left(-B \frac{\sin^2 \theta}{\lambda^2}\right)$ where the parameter B , the isotropic temperature factor, is equal to $8\pi^2 \overline{u^2}$, $\overline{u^2}$ being the mean square displacement of the atoms from their mean positions.

By using the method introduced by A.G.C. Wilson¹⁰ one can obtain an overall value of B , and at the same time, places all the observed intensities on an approximately absolute basis.

Wilson showed that average absolute structure factor depends only on what is in the cell and not where the atoms are located and hence for a random distribution of N atoms in the unit cell

$$\langle |F|^2 \rangle = \sum_{j=1}^N f_j^2 \quad (12)$$

Dividing entire reciprocal space observed into annular zones of equal S^2 ($S = \sin\theta/\lambda$), $\langle |F_{\text{obs}}|^2 \rangle$ is determined from each of them

and $\sum_{j=1}^N f_{oj}^2 (S_{mid})$ is calculated using the mean value of S^2 for each zone. Since $|F_{obs}|^2$ is usually known on an arbitrary scale, we may write

$$\langle |F_{obs}|^2 \rangle = K \langle |F|^2 \rangle \quad (13)$$

where $\langle |F| \rangle$ is the average absolute structure factor. To separate out thermal motion in the crystal, we write

$$\langle |F|^2 \rangle = \sum_{j=1}^N f_j^2 = \sum_{j=1}^N f_{oj}^2 \exp(-2B_j S^2) \quad (14)$$

Assuming B same for all atoms

$$\langle |F| \rangle^2 = \exp(-2B S^2) \sum_{j=1}^N f_{oj}^2 \quad (15)$$

Substituting the Eqn. (15) in Eqn. (13) we get,

$$\langle |F_{obs}|^2 \rangle = K \exp(-2B S^2) \sum_{j=1}^N f_{oj}^2$$

$$\ln \frac{\langle |F_{obs}|^2 \rangle}{\sum_{j=1}^N f_{oj}^2} = \ln K - \frac{2B \sin^2 \theta}{\lambda^2} \quad (16)$$

The plot of $\frac{\ln \langle |F_{\text{obs}}|^2 \rangle}{\sum_{j=1}^N f_{oj}^2}$ against $\frac{\sin^2 \theta}{\lambda^2}$ called the Wilson plot

is, therefore, a straight line except for the scatter due to experimental errors and furnishes us with intercept of $\ln K$ and a slope of $-2B$.

When instead of random distribution of atoms, groups of atoms with known geometry (such as benzene ring) are present in the structure, they may be included in the expression for average intensity even knowing nothing about their positions and orientations. When G groups of known geometry are present, the k^{th} of which contains M_k atoms, we may write using the scattering formula of Debye¹¹

$$\langle |F|^2 \rangle = \sum_{k=1}^G \sum_{i=1}^{M_k} \sum_{j=1}^{M_k} f_i f_j \frac{\sin 2\pi r_{ij} S}{2\pi r_{ij} S} + \sum_{j=1}^N f_j^2 \quad (17)$$

where r_{ij} is the distance between the i^{th} and j^{th} atoms of the k^{th} group and $S = S_{\text{mid}}$ as before. The plot in this case is known as Debye plot and gives a better straight line fit for obtaining B and k .

It is often advantageous to use a k -curve. For this purpose, $k(S_{\text{mid}})$ is computed for each zone of S^2 mentioned above, as

$$k(S_{\text{mid}}) = \frac{\sum \epsilon \sum_{j=1}^N f_{oj}(S)}{\sum |F_o|^2(S)} \quad (18)$$

where ϵ is a small integer depending on the space group¹². A least

squares procedure is used to fit a best smooth analytical functions, usually $\ln k = A + B S^c$ to experimental points. When $c = 2.0$, the curve is the same as Wilson's plot.

After scaling the data and estimating the temperature factors we try to postulate a trial structure by direct methods.

4.5. Unitary and Normalized Structure Factors

For direct methods it is an advantage to work with structure factors for which the fall off with increasing scattering angle has been removed. The unitary structure factor is defined as

$$U(\vec{h}) = \frac{F(\vec{h})}{\sum_{j=1}^N f_j} \quad \text{so that } |U(\vec{h})| \leq 1.$$

Writing the unitary scattering factor as

$$n_j = \frac{f_j}{\sum_{j=1}^N f_j}$$

we may write

$$U(\vec{h}) = \sum_{j=1}^N n_j \exp 2\pi i (\vec{h} \cdot \vec{r}_j) \quad (19)$$

Another corrected structure factor of great theoretical importance is the normalized structure factor given by

$$|E(\vec{h})|^2 = \frac{|F(\vec{h})|^2}{\varepsilon(\vec{h}) \sum_{j=1}^N f_j^2}$$

where $\varepsilon(\vec{h})$ takes into account the effect of space group symmetry.

Now if \hat{f} be the common shape for all atoms then $f_j = Z_j \hat{f}$.

$$E(\vec{h}) = \varepsilon(\vec{h})^{-1/2} \frac{F(\vec{h})}{\left(\sum_{j=1}^N Z_j^2 \hat{f}^2 \right)^{1/2}} = \varepsilon(\vec{h})^{-1/2} \sum_{j=1}^N \left(\frac{Z_j}{\sigma_2^{1/2}} \right) \exp 2\pi i(\vec{h} \cdot \vec{r}_j)$$

(20)

where $\sigma_m = \sum Z_j^m$. $E(\vec{h})$ is called the normalized structure factors because of its property $\langle |E(\vec{h})|^2 \rangle = 1$. This relationship shows that the average of E^2 can be carried out regardless of θ . The same is not true, however, of either $|F(\vec{h})|^2$ or $|U(\vec{h})|^2$ and this simplification is one of the main reasons why E 's are preferred for use in direct methods.

Some Relations Involving the Magnitudes and the Phases :

Harker-Kasper Inequalities:

In 1948 Harker and Kasper¹³ using Cauchy inequality relation derived the following inequality relation between magnitudes and phases of unitary structure factors,

$$U(\vec{h})^2 \leq 1/2 [1 + U(2\vec{h})] \quad (21)$$

If we denote the sign of $U(\vec{h})$ by $S(\vec{h})$ which can have the values either +1 or -1, then this relationship can be written as

$$S(\vec{h}) S(\vec{h}') S(\vec{h} + \vec{h}') = 1$$

A development made by Karle and Hauptman¹⁴ in the form of an inequality does depend on the non-negativity of electron density. For a centro symmetric structure where $U(\vec{h}) = U(-\vec{h})$ gives

$$1 - U(\vec{h})^2 - U(\vec{k})^2 - U(\vec{h}-\vec{k})^2 + 2U(\vec{h}) U(\vec{k}) U(\vec{h}-\vec{k}) \geq 0$$

from which, if the U's are sufficiently large, it may be shown that

$$S(\vec{h}) S(\vec{k}) S(\vec{h} - \vec{k}) = 1$$

A significant step in the development of direct methods was done by Sayre¹⁵.

The electron density is given by the summation

$$\rho(\vec{r}) = 1/V \sum_{\vec{h}} F(\vec{h}) \exp -2\pi i(\vec{h} \cdot \vec{r})$$

and we may write

$$\rho(\vec{r})^2 = 1/V \sum_{\vec{h}} G(\vec{h}) \exp -2\pi i(\vec{h} \cdot \vec{r})$$

where $G(\vec{h})$ is the Fourier coefficient of the squared density.

If the structure consists of equal resolved atoms, then both $\rho(\vec{r})$

and $\rho(\vec{r})^2$ will show equal resolved peaks. If the scattering factors of the squared atoms is represented by g and that of the normal atoms by f then

$$F(\vec{h}) = \frac{f}{gV} \sum_{\vec{h}'} F(\vec{h}') F(\vec{h} - \vec{h}') \quad (22)$$

This is Sayre's equation and is an exact relationship between structure factors for equal and resolved atoms.

For a centrosymmetric structure it might be assumed that a large product on the right hand side of Eqn. (22) was likely to have the same sign as $F(\vec{h})$. This leads to the relationship that for large structure factors

$$S(\vec{h}) S(\vec{h}') S(\vec{h} - \vec{h}') \approx +1 \quad (23)$$

This was the sign relationship given in the papers by Cochran¹⁶ and Zachariason¹⁷. Expressions for the probability of Eqn. (23) was given by Cochran and Woolfson¹⁸. This is for an equal atom structure

$$P_+ = 1/2 + 1/2 \tanh \left[\frac{N^{1/2}}{E(\vec{h})} E(\vec{h}') E(\vec{h} - \vec{h}') \right] \quad (24)$$

where P_+ is the probability that the product of signs in Eqn. (4.25) is positive.

This expression also gives the probability that $S(\vec{h})$ equals the signs $S(\vec{h}') S(\vec{h} - \vec{h}')$. If there are several pairs of known signs all contributing to the indication of new one then the probability for

the new sign being +ve will be

$$P_+(\vec{h}) = 1/2 + 1/2 \tanh \left[N^{-1/2} \left| E(\vec{h}) \sum_{\vec{h}'} E(\vec{h}) E(\vec{h} - \vec{h}') \right| \right] \quad (25)$$

In Eqns. (24) and (25) if the atoms are not equal then $N^{-1/2}$ is replaced by $\sigma_3 \sigma^{-3/2}$ where $\sigma_n = \sum_j Z_j^n$, Z_{ij} being the atomic number of the j^{th} atom. The approximate phases thus obtained have to be refined and this may be conveniently done by using following tangent formula of Karle and Hauptman¹⁴

$$\tan \phi(\vec{h}) = \frac{\sum_{\vec{k}} K(\vec{h}, \vec{k}) \sin[\phi(\vec{h}-\vec{k}) + \phi(\vec{k})]}{\sum_{\vec{k}} K(\vec{h}, \vec{k}) \cos[\phi(\vec{h}-\vec{k}) + \phi(\vec{k})]} \quad (26)$$

A quantity $\alpha(\vec{h})$ which gives a measure of the reliability with which $\phi(\vec{h})$ may be determined was defined by Karle and Karle¹⁹

$$\alpha(\vec{h})^2 = \left[\sum_{\vec{k}} K(\vec{h}, \vec{k}) \sin[\phi(\vec{h}-\vec{k}) + \phi(\vec{k})] \right]^2 + \left[\sum_{\vec{k}} K(\vec{h}, \vec{k}) \cos[\phi(\vec{h}-\vec{k}) + \phi(\vec{k})] \right]^2 \quad (27)$$

All the theory given above is the launching pad from which modern direct methods have grown to the present form.

Structure Invariant and Semi Invariant

A structure invariant is defined as a quantity which is independent of the choice of origin in the unit cell.

The intensities of reflections, $|F(\vec{h})|^2$'s are structure invariants. However, the structure factor itself is not structure invariant. Otherwise the phase problem would not exist in crystallography. The structure factor $F(\vec{h})$ is given by

$$F(\vec{h}) = |F(\vec{h})| \exp i\phi(\vec{h}) = \sum_{j=1}^N f_j \exp 2\pi i(\vec{h} \cdot \vec{r}_j) \quad (28)$$

With shift Δr of the origin, the Eqn. (28) changes to

$$\begin{aligned} F'(\vec{h}) &= \sum f_j \exp 2\pi i[\vec{h} \cdot (\vec{r}_j - \Delta\vec{r})] \\ &= |F(\vec{h})| \exp -2\pi i(\vec{h} \cdot \Delta\vec{r}) \exp i\phi(\vec{h}) \end{aligned} \quad (29)$$

Thus we see that the phase changes by $-2\pi i(\vec{h} \cdot \Delta\vec{r})$ while the amplitude is invariant.

In a similar way it can be shown that $|F(\vec{h})|^2$ is structure invariant.

Individual phases depend on the structure and choice of origin, some combinations of them is a structure invariant. For example if $h_1 + h_2 + h_3 = 0$ then $\phi(\vec{h}_1) + \phi(\vec{h}_2) + \phi(\vec{h}_3)$ is a structure invariant for every space group. It follows directly from the fact that $F(\vec{h}) F(\vec{k}) F(-\vec{h}-\vec{k})$ is an invariant :

$$\begin{aligned} F'(\vec{h}) F'(\vec{k}) F'(-\vec{h}-\vec{k}) &= F(\vec{h}) \exp -2\pi i(\vec{h} \cdot \Delta\vec{r}) F(\vec{k}) \exp -2\pi i(\vec{k} \cdot \Delta\vec{r}) \\ &\quad F(-\vec{h}-\vec{k}) \exp 2\pi i[(\vec{h} \cdot \Delta\vec{r}) + (\vec{k} \cdot \Delta\vec{r})] \\ &= F(\vec{h}) F(\vec{k}) F(-\vec{h}-\vec{k}) \end{aligned} \quad (30)$$

Since the moduli of the structure factors are invariant themselves,

the angular part of $F(\vec{h}) F(\vec{k}) F(-\vec{h}-\vec{k})$ is also an invariant i.e., $\phi(\vec{h}) + \phi(\vec{k}) + \phi(-\vec{h}-\vec{k})$ is an invariant or $\phi_3 = \phi(h) + \phi(k) + \phi(-h-k)$ is an invariant.

Knowledge of the actual values of ϕ_3 or reliable estimates of ϕ_3 would strengthen direct method procedures enormously. Instead direct methods mostly use $|\phi_3| = 0$ for large values of $E_3 = N - 1/2 |E(h) E(k) E(-h-k)|$

The structure-semi-invariants are quantities which do not change value by transfer from one special origin to another. The structure-semi-invariants originate from space group symmetry. For $P\bar{1}$, $F(2\vec{h})$, $F(\vec{h}+\vec{k})$, $F(\vec{h}-\vec{k})$ are semi-invariants. Structure-semi-invariants are crucial to origin and enantiomorph specializations on which many methods depend for initiating phase determination.

There are various direct method package programs which are used for the solution of crystal structures. These are as MULTAN²⁰, SHELX²¹ and SIMPEL²² XTAL²³, SAPI²⁴, X-RAY²⁵, RATAN²⁶.

Here the structure has been solved by the direct method program SIMPEL.

The program system SIMPEL devoted to the symbolic addition method, is a complete direct method system, which may enter with $|F|$ and may produce an E-map of the structures. The unique part of SIMPEL is formed by a series of routines, successively gathering the relationships and determining a starting set, carrying out a symbolic addition, finding the correct numerical values for the symbols and finally executing a numerical phase extension and refinement.

In a symbolic addition the following expressions play important roles.

The Triplet Relation:

$$\phi(\vec{H}) \cong \phi(\vec{K}) + \phi(\vec{H} - \vec{K}) \text{ for large value of } E_3 = N^{1/2} \left| \left[E(\vec{H}) E(\vec{K}) E(\vec{H} - \vec{K}) \right] \right|.$$

In a centrosymmetric case, the triplet relation becomes

$$S(\vec{H}) \approx S(\vec{K}) S(\vec{H} - \vec{K})$$

in which S is the sign of a reflection.

These formulae have their counter parts when more than one reflection are available.

$$\phi(\vec{H}) = \frac{\sum_{\vec{K}} E_3 \left[\phi(\vec{K}) + \phi(\vec{H} - \vec{K}) \right]}{\sum_{\vec{K}} E_3}$$

$$\text{and } S(\vec{H}) = A \sum E_3 S(\vec{K}) S(\vec{H} - \vec{K}).$$

In general, in the final stage of a symbolic addition numerical phases has to be refined. This is carried out by means of the tangent formula or rather, because phases must be known on the interval $0 \leq \phi \leq 2\pi$ by its exponential analogue,

$$\exp i\phi(\vec{H}) = \frac{\sum_{\vec{k}} E_3 \exp i[\phi(\vec{H}) + \phi(\vec{H}-\vec{k})]}{\left| \sum_{\vec{k}} E_3 \exp i[\phi(\vec{H}) + \phi(\vec{H}-\vec{k})] \right|}$$

Elements of a Symbolic Addition:

Calculation of the normalized structure factors

In the first step the experimental structure factor data are corrected for thermal motion (Wilson plot, Debye curve, K curve), brought to absolute scale and finally converted into normalized structure factors $|E|$.

Generation of the Phase Relationships:

The phase relationships are collected. In the program system SIMPEL not only triplet relations are generated, but also positive and negative quartets relationship, Harker-Kasper relations and quintets are also generated.

$$\sum_1 \text{Relation}^{27} :$$

The positive quartet relation is formulated²⁸ as $\phi(\vec{H}) + \phi(\vec{K}) + \phi(\vec{L}) + \phi(-\vec{H} - \vec{K} - \vec{L}) \approx 0$ for large value of $E_4 = N^{-1} |E(\vec{H}) E(\vec{K}) E(\vec{L}) E(-\vec{H} - \vec{K} - \vec{L})|$ and large $|E(\vec{H} + \vec{K})|$, $|E(\vec{H} + \vec{L})|$ and $|E(\vec{K} + \vec{L})|$.

Negative Quartet Relation²⁹:

$\phi(\vec{H}) + \phi(\vec{K}) + \phi(\vec{L}) + \phi(-\vec{H} - \vec{K} - \vec{L}) \approx \pi$ for reasonably large values of E_4 and small $|E(\vec{H} + \vec{K})|$, $|E(\vec{H} + \vec{L})|$ and $|E(\vec{K} + \vec{L})|$.

Harker-Kasper Relations³⁰:

Using the probability that the product $S(\vec{H} + \vec{K}) \times S(\vec{H} - \vec{K})$ is negative, the larger $|E(\vec{H})|$, $|E(\vec{H} + \vec{K})|$, $|E(\vec{H} - \vec{K})|$ and the smaller $|E(\vec{K})|$, $|E(2\vec{H})|$. Of course this is the result of a special negative quartet, the main terms being $E(\vec{H})$, $E(\vec{K})$, $E(\vec{H} + \vec{K})$ and $E(\vec{H} - \vec{K})$.

Quintets:

From the general Hughes formula derived by Simerska³¹ the quintet phase relation can be written as

$$\phi(\vec{H}) + \phi(\vec{K}) - \phi(\vec{L}) - \phi(\vec{M}) - \phi(-\vec{H} - \vec{K} - \vec{L} - \vec{M}) \simeq \pi.$$

In a first approximation π is expected to be zero for large values of

$$E_5 = N^{-3/2} |E(\vec{H}) E(\vec{K}) E(\vec{L}) E(\vec{M}) E(-\vec{H} - \vec{K} - \vec{L} - \vec{M})|.$$

Starting Set Determination:

The determination of the starting set begins with a convergence procedure similar to that devised by Germain, Main and Woolfson³². This procedure searches for that reflection which is the weakest linked to the other reflections by means of the phase relations and then this reflection is removed from the set of reflections. At the same time all its phase relations are removed from the collection of phase relationships. This process is repeated until no reflections are left in the set. Any time the reflection is removed without having phase relationships linking it with other phases, this reflection has taken to be starting set. Since a starting set reflections with large $|E|$ are preferred, the use of triplets and

quartets generally leads to very good starting set. The second set is a few cycles of symbolic addition using quartets and triplets, employing very strict acceptance criteria, not allowing relations among the symbolic phases. This leads to a much larger starting set.

The next step is the extension of starting set. This is done in SIMPEL using triplet relations only. It is very essential that no errors are included during this process and therefore, the criteria used to accept a symbolic phase for a reflection are very strict, in particular in the beginning. In general, no single indication will be accepted unless it belongs to the ten to fifteen strongest triplet relationships. For multiple indications giving rise to the symbolic phase, high acceptance limits are applied. In general this precautions make sure that the resulting set of symbolic phases contains the correct solution.

Numerical Values for the Symbols :

Figures of Merit

With the extended group of phased reflections as input numerical values for the symbols are calculated using a number of figures of merit (FOM's).

In general figures of merit can be based on any quantity which can be expected to be extreme for the set of correct signs. In SIMPEL several FOM's may be used.

- 1) \sum_2 - consistency FOM³³
- 2) The positive quartet criterion (PQC)³⁴
- 3) The negative quartet criterion (NQC)³⁴

4) The \sum_1 - criterion³⁵

5) The Harker-Kasper criterion³⁶

Apart from the separate FOM's also a combined FOM is calculated, which mostly discriminates the correct solution without difficulties.

After determining the symbols all symbolically phased relations can get numerical phase. These phases are then used as starting point for numerical phase extension, because in general the number of phased reflections is yet insufficient to calculate a good E map. In the centrosymmetric case this is achieved by means of a fast \sum_2 refinement and extension. In the case of non centrosymmetric usual tangent refinement is used.

Thus SIMPEL produces a set of E values with phases, which can be fed into an E map calculating program with subsequent interpretation.

Eventually the atomic positions can be tested and be refined by a fast diagonal least squares program.

4.6 Structure Determination and Refinement

The structure was determined by means of the direct methods program SIMPEL 83 of Kiers and Schenk²³, using all reflections in order to employ positive and negative quartet relationships, signal reflections and special two dimensional quartets, apart from the triplets. The strongest 500 reflections were phased using three symbols. Two out of eight solutions had appreciably better combined figures of merit. The E-map with largest combined figure of merit could not solve the structure and showed instead a superposition of

two structures. The other one revealed the structure completely.

The trial structure was found to have an R value 0.30, which after four cycles of refinement, reduced to 0.152 (using first an overall value and then individual values for isotropic temperatures factors). The hydrogen atoms were found in a ΔF synthesis. The hydrogen atoms were given isotropic temperatures factors and non-hydrogen atoms anisotropic temperatures factors. Then the structure was refined through several cycles by block diagonal least squares. A weighting scheme $w = (7.9 + F_{obs} + 0.0049 F_{obs}^2)^{-1}$ was applied and extinction was taken into account with $ext. = 0.85$. Finally R value converged to 0.041 ($R_w = 0.04$). All the calculations were carried out with X-ray 76 program of Stewart²⁶ using scattering factors from Cromer and Mann³⁷.

4.7. Results and Discussions :

4.7.1. Molecular Conformations

Crystallographic data of the sample is given in Table 4.1. Final positions and thermal parameters of the atoms are listed in Tables 4.2-4.4 using the atom numbering of Fig. 4.1. Bond lengths and bond angles are given in Tables 4.5 and 4.6. The perspective drawing of the molecule viewed normal to its least squares plane is shown in Fig. 4.1. Newman projections along different C-C bonds are shown in Fig. 4.2.

The average C-C bond length in the phenyl ring ($C_{18}-C_{23}$) is $1.385(2) \text{ \AA}$. In the pyrimidine ring (C_7-N_2) the average C-C bond length is $1.386(2) \text{ \AA}$ and the C-N bond length is $1.335(2) \text{ \AA}$. The average C-C bond length in the cyclohexane ring (C_8-C_{12}) is $1.524(2) \text{ \AA}$. All lengths are consistent with our previous

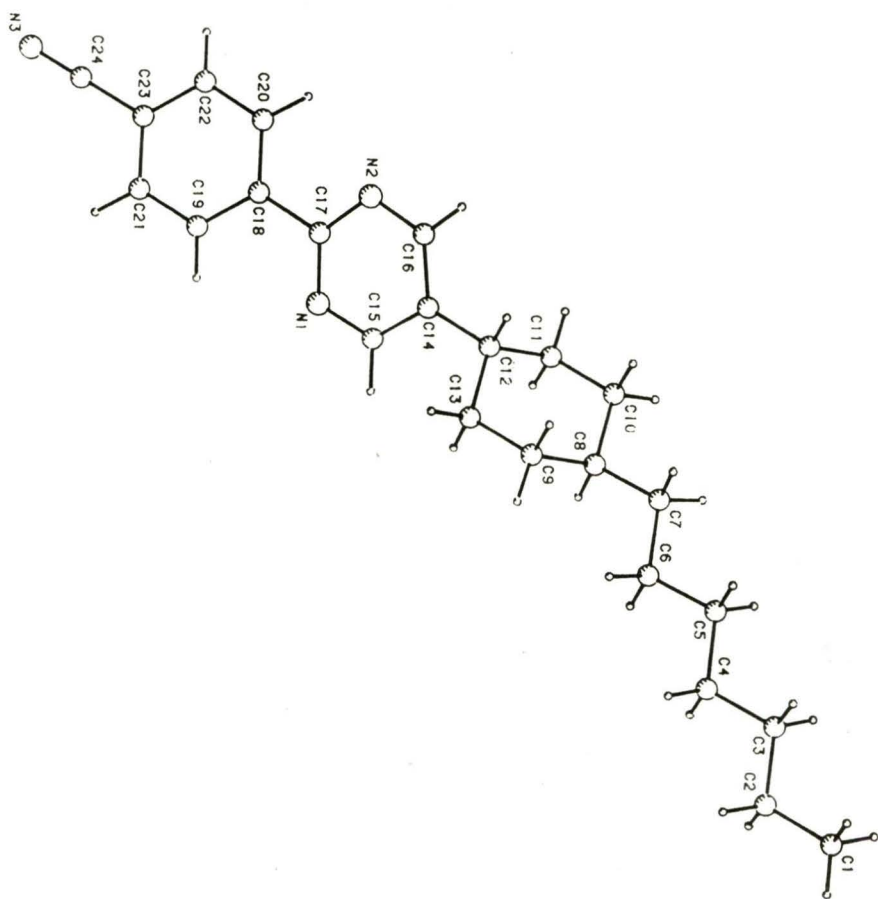


Fig. 4.1

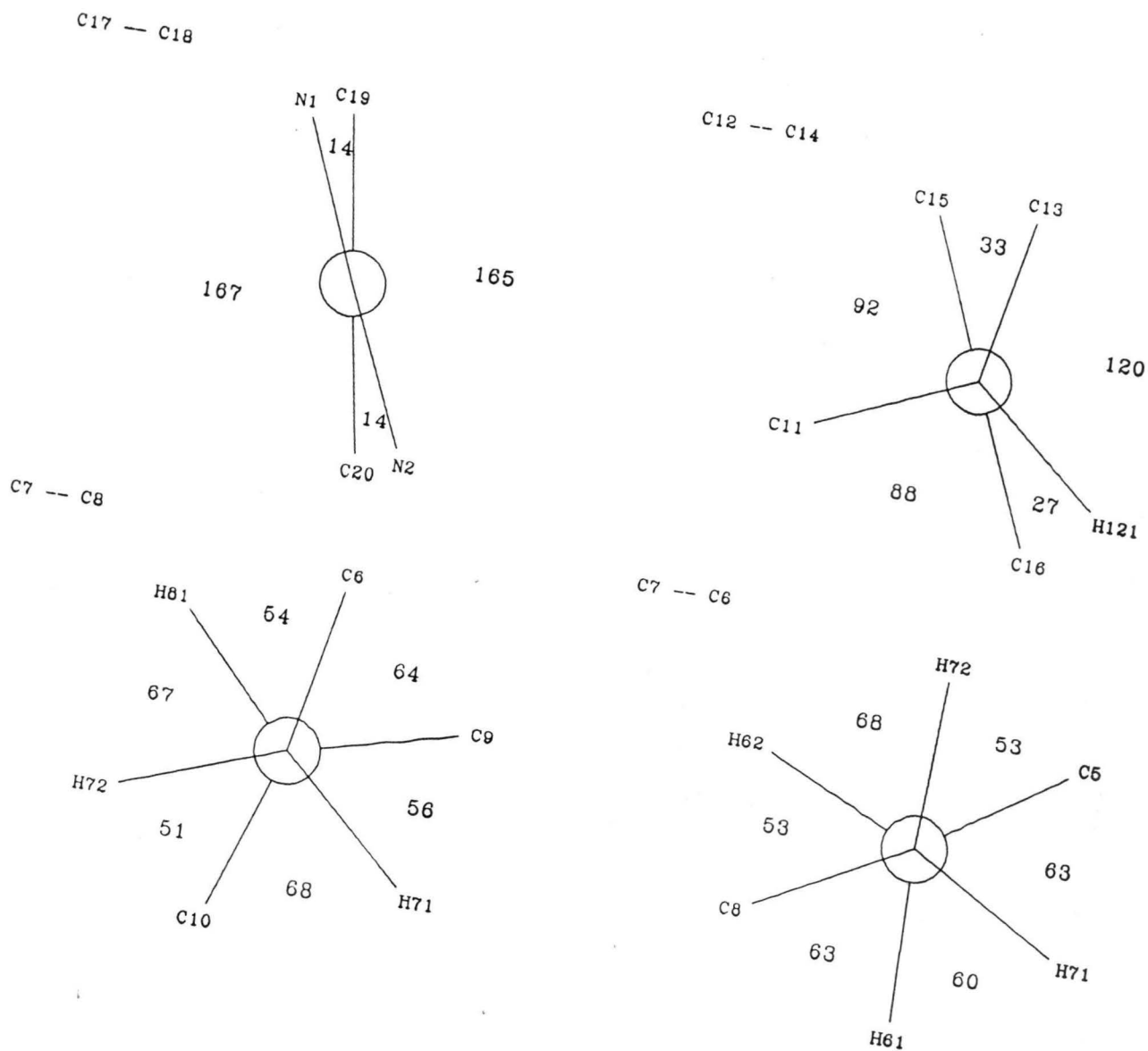


Fig. 4.2

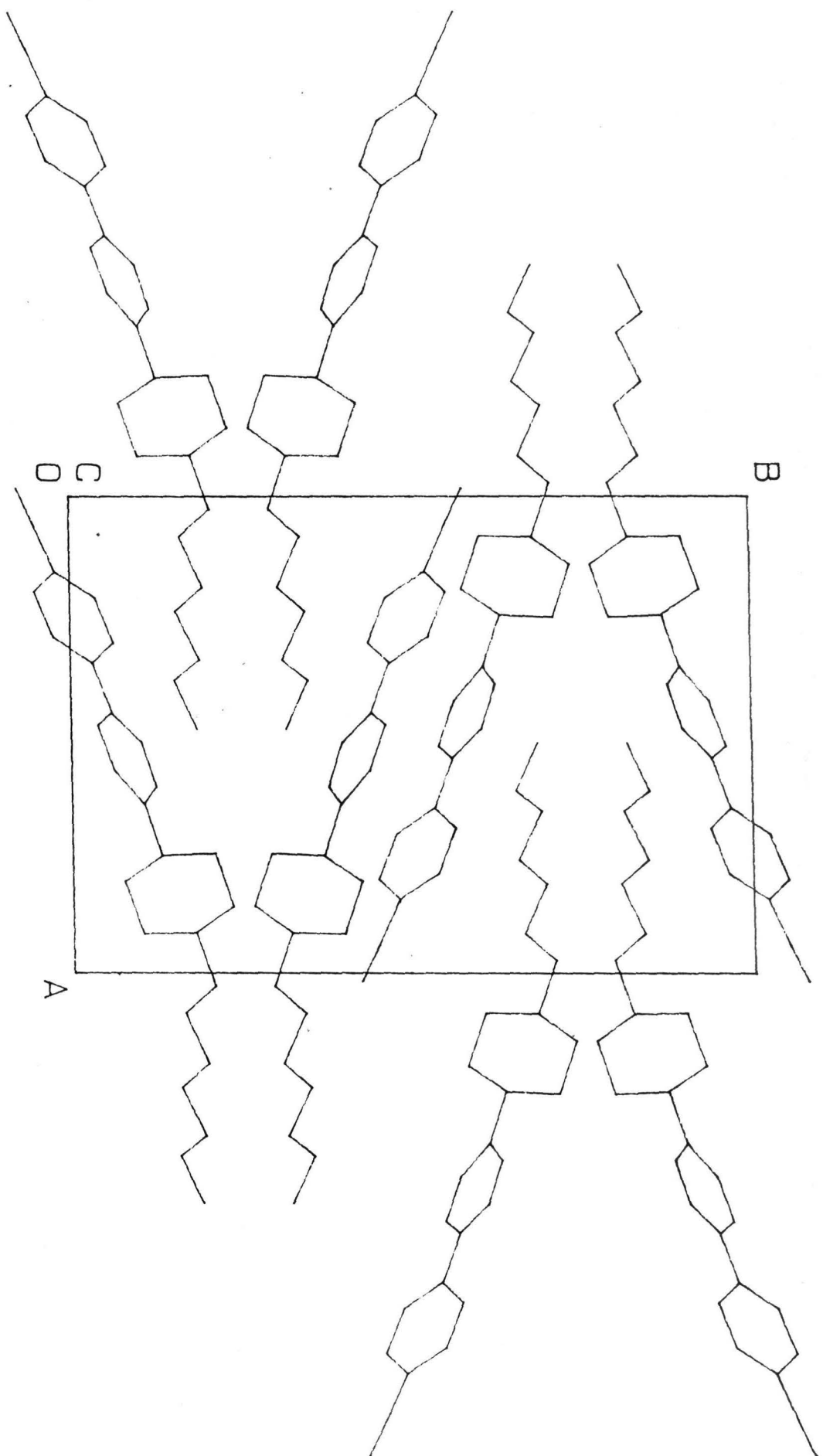


Fig. 4.3

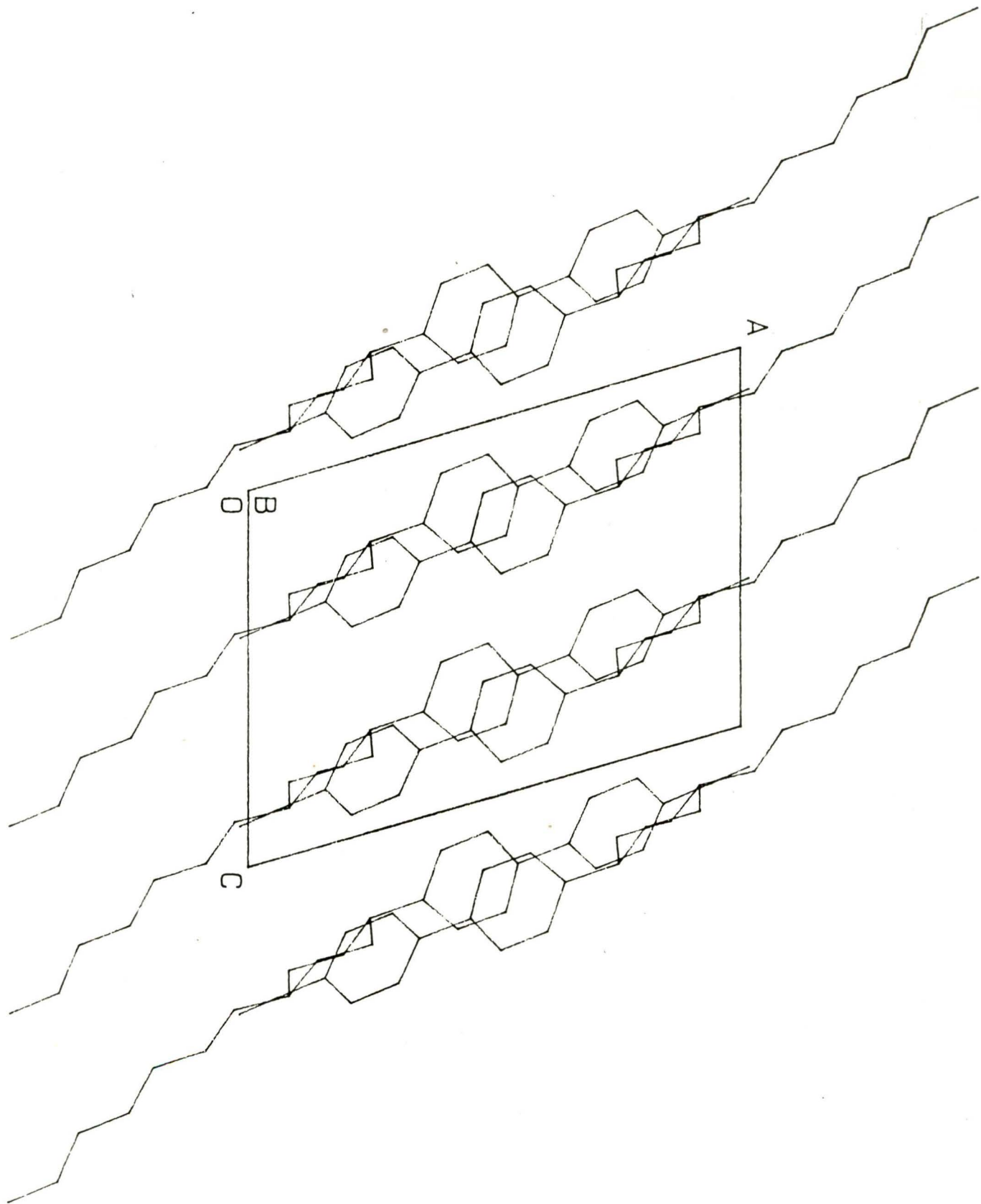


Fig. 4.5

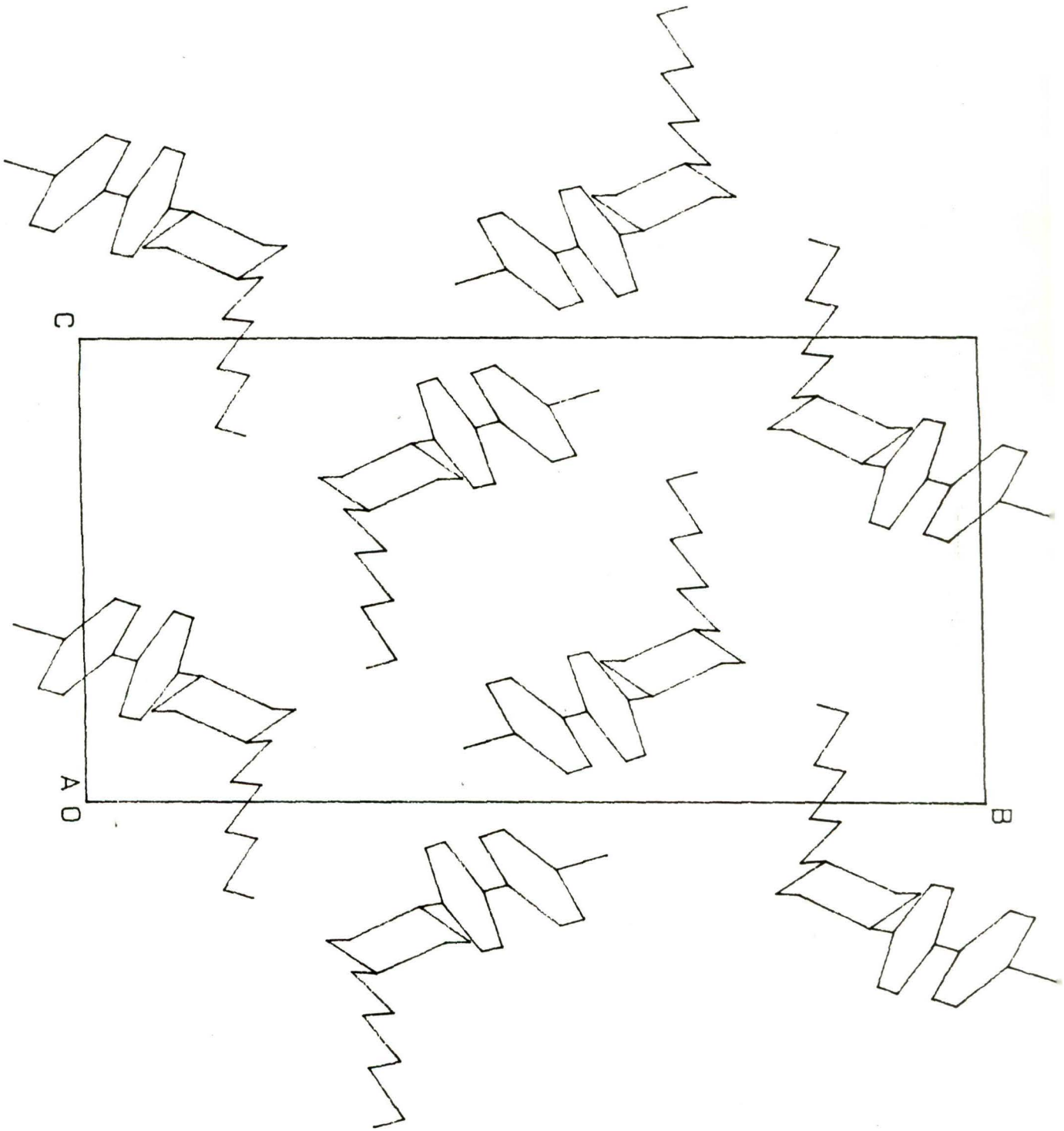


Table 4.2

Fractional co-ordinates of the non-hydrogen atoms
and equivalent isotropic thermal parameters.

	X	Y	Z	Ueq
C(1)	1.4855(2)	0.1849(2)	-0.2097(3)	0.094(2)
C(2)	1.3837(2)	0.1515(1)	-0.1916(2)	0.076(1)
C(3)	1.3414(1)	0.1899(1)	-0.0794(2)	0.064(1)
C(4)	1.2392(1)	0.1545(1)	-0.0645(2)	0.066(1)
C(5)	1.1889(1)	0.1956(1)	0.0369(2)	0.063(1)
C(6)	1.0834(1)	0.1612(1)	0.0432(2)	0.063(1)
C(7)	1.0267(1)	0.2074(1)	0.1319(2)	0.063(1)
C(8)	0.9146(1)	0.17944(9)	0.1271(2)	0.0525(9)
C(9)	0.9169(1)	0.1018(1)	0.1954(2)	0.062(1)
C(10)	0.8578(2)	0.2351(1)	0.1999(2)	0.066(1)
C(11)	0.7469(1)	0.2085(1)	0.2014(2)	0.063(1)
C(12)	0.7523(1)	0.1311(1)	0.2732(2)	0.0523(9)
C(13)	0.8061(1)	0.0752(1)	0.1967(2)	0.064(1)
C(14)	0.6440(1)	0.10520(9)	0.2812(2)	0.0501(8)
C(15)	0.5729(1)	0.0620(1)	0.1760(2)	0.061(1)
C(16)	0.6077(1)	0.1235(1)	0.3991(2)	0.060(1)
C(17)	0.4525(1)	0.05958(9)	0.3051(2)	0.0508(9)
C(18)	0.3485(1)	0.03229(9)	0.3196(2)	0.0498(9)
C(19)	0.2930(1)	-0.0253(1)	0.2311(2)	0.063(1)
C(20)	0.3058(1)	0.0632(1)	0.4237(2)	0.059(1)
C(21)	0.1980(1)	-0.0523(1)	0.2468(2)	0.063(1)
C(22)	0.2105(1)	0.0363(1)	0.4401(2)	0.060(1)
C(23)	0.1567(1)	-0.02153(9)	0.3522(2)	0.0522(9)
C(24)	0.0591(1)	-0.0526(1)	0.3705(2)	0.0562(9)
N(1)	0.4779(1)	0.03849(9)	0.1857(1)	0.0606(9)
N(2)	0.5133(1)	0.10179(9)	0.4130(2)	0.0606(9)
N(3)	-0.0171(1)	-0.07846(9)	0.3854(2)	0.069(1)

Table 4.3

Fractional co-ordinates and isotropic thermal parameters
of the hydrogen atoms.

	X	Y	Z	U
H(11)	1.541(2)	0.184(1)	-0.114(3)	0.118(8)
H(12)	1.515(2)	0.160(2)	-0.280(3)	0.139(9)
H(13)	1.474(2)	0.243(2)	-0.235(3)	0.14(1)
H(21)	1.320(2)	0.155(1)	-0.294(2)	0.115(8)
H(22)	1.390(2)	0.096(1)	-0.169(2)	0.106(7)
H(31)	1.402(2)	0.190(1)	0.023(2)	0.097(7)
H(32)	1.328(1)	0.243(1)	-0.106(2)	0.077(6)
H(41)	1.254(1)	0.100(1)	-0.035(2)	0.080(6)
H(42)	1.185(1)	0.153(1)	-0.166(2)	0.082(6)
H(51)	1.239(1)	0.198(1)	0.134(2)	0.081(6)
H(52)	1.175(1)	0.248(1)	0.006(2)	0.075(5)
H(61)	1.096(1)	0.108(1)	0.083(2)	0.077(6)
H(62)	1.035(1)	0.155(1)	-0.061(2)	0.084(6)
H(71)	1.074(1)	0.208(1)	0.233(2)	0.071(5)
H(72)	1.019(2)	0.263(1)	0.093(2)	0.088(6)
H(81)	0.867(1)	0.175(1)	0.019(2)	0.063(5)
H(91)	0.968(1)	0.106(1)	0.302(2)	0.085(6)
H(92)	0.950(1)	0.063(1)	0.145(2)	0.084(6)
H(101)	0.906(1)	0.242(1)	0.304(2)	0.079(6)
H(102)	0.856(1)	0.285(1)	0.158(2)	0.082(6)
H(111)	0.697(1)	0.203(1)	0.099(2)	0.076(6)
H(112)	0.714(1)	0.245(1)	0.253(2)	0.082(6)
H(121)	0.798(1)	0.138(1)	0.373(2)	0.063(5)
H(131)	0.816(1)	0.024(1)	0.248(2)	0.082(6)
H(132)	0.760(1)	0.071(1)	0.093(2)	0.076(5)
H(151)	0.592(1)	0.045(1)	0.087(2)	0.077(6)
H(161)	0.654(1)	0.155(1)	0.481(2)	0.077(6)
H(191)	0.323(1)	-0.046(1)	0.157(2)	0.083(6)
H(201)	0.346(1)	0.106(1)	0.485(2)	0.083(6)
H(211)	0.157(1)	-0.093(1)	0.183(2)	0.083(6)
H(221)	0.178(1)	0.058(1)	0.507(2)	0.081(6)

Table 4.4

Anisotropic thermal parameters.

	U11	U22	U33	U12	U13	U23
C(1)	0.073(1)	0.130(2)	0.087(2)	-0.010(1)	0.038(1)	-0.007(1)
C(2)	0.070(1)	0.078(1)	0.087(1)	-0.003(1)	0.036(1)	-0.013(1)
C(3)	0.063(1)	0.070(1)	0.062(1)	-0.0062(9)	0.0207(8)	-0.0055(9)
C(4)	0.060(1)	0.067(1)	0.073(1)	-0.0046(9)	0.0232(9)	-0.0070(9)
C(5)	0.060(1)	0.069(1)	0.062(1)	-0.0071(9)	0.0206(8)	-0.0043(9)
C(6)	0.058(1)	0.064(1)	0.069(1)	-0.0037(8)	0.0245(9)	-0.0017(9)
C(7)	0.061(1)	0.066(1)	0.066(1)	-0.0094(8)	0.0242(8)	-0.0077(8)
C(8)	0.0550(9)	0.0517(9)	0.0516(9)	-0.0011(7)	0.0170(7)	0.0002(7)
C(9)	0.058(1)	0.057(1)	0.076(1)	0.0069(8)	0.0288(9)	0.0078(9)
C(10)	0.070(1)	0.050(1)	0.086(1)	-0.0055(8)	0.034(1)	-0.0072(9)
C(11)	0.061(1)	0.051(1)	0.082(1)	0.0038(8)	0.0287(9)	-0.0001(9)
C(12)	0.0488(8)	0.060(1)	0.0478(8)	0.0008(7)	0.0140(7)	0.0025(7)
C(13)	0.064(1)	0.0501(9)	0.084(1)	0.0030(8)	0.0333(9)	0.0051(9)
C(14)	0.0510(8)	0.0511(9)	0.0482(8)	0.0037(7)	0.0148(7)	0.0036(7)
C(15)	0.062(1)	0.076(1)	0.0504(9)	-0.0077(9)	0.0242(8)	-0.0074(8)
C(16)	0.0565(9)	0.068(1)	0.057(1)	-0.0069(8)	0.0192(8)	-0.0127(8)
C(17)	0.0538(9)	0.0523(9)	0.0478(8)	0.0013(7)	0.0172(7)	-0.0001(7)
C(18)	0.0535(9)	0.0521(9)	0.0454(8)	0.0009(7)	0.0172(7)	0.0003(7)
C(19)	0.067(1)	0.072(1)	0.055(1)	-0.0091(9)	0.0276(8)	-0.0133(8)
C(20)	0.061(1)	0.061(1)	0.061(1)	-0.0075(8)	0.0255(8)	-0.0126(8)
C(21)	0.065(1)	0.068(1)	0.059(1)	-0.0140(9)	0.0223(8)	-0.0142(9)
C(22)	0.061(1)	0.063(1)	0.064(1)	-0.0035(8)	0.0288(8)	-0.0112(8)
C(23)	0.0514(9)	0.0529(9)	0.0536(9)	0.0009(7)	0.0178(7)	0.0038(7)
C(24)	0.0568(9)	0.0533(9)	0.059(1)	0.0005(7)	0.0187(8)	-0.0016(8)
N(1)	0.0590(8)	0.077(1)	0.0504(8)	-0.0110(7)	0.0231(6)	-0.0100(7)
N(2)	0.0580(8)	0.0686(9)	0.0593(8)	-0.0086(7)	0.0239(7)	-0.0142(7)
N(3)	0.0635(9)	0.068(1)	0.081(1)	-0.0092(7)	0.0292(8)	-0.0073(8)

Table 4.5

Bond distances of the non-hydrogen atoms (A)
with standard deviations in parentheses.

C(1)	-	C(2)	1.510(3)	C(14)	-	C(16)	1.388(3)
C(2)	-	C(3)	1.510(3)	C(15)	-	N(1)	1.337(2)
C(3)	-	C(4)	1.518(3)	C(16)	-	N(2)	1.333(2)
C(4)	-	C(5)	1.513(3)	C(17)	-	C(18)	1.485(2)
C(5)	-	C(6)	1.522(3)	C(17)	-	N(1)	1.336(2)
C(6)	-	C(7)	1.521(3)	C(17)	-	N(2)	1.333(2)
C(7)	-	C(8)	1.532(3)	C(18)	-	C(19)	1.387(2)
C(8)	-	C(9)	1.522(2)	C(18)	-	C(20)	1.392(3)
C(8)	-	C(10)	1.523(3)	C(19)	-	C(21)	1.378(3)
C(9)	-	C(13)	1.525(3)	C(20)	-	C(22)	1.384(3)
C(10)	-	C(11)	1.525(3)	C(21)	-	C(23)	1.390(3)
C(11)	-	C(12)	1.528(2)	C(22)	-	C(23)	1.381(2)
C(12)	-	C(13)	1.523(3)	C(23)	-	C(24)	1.445(3)
C(12)	-	C(14)	1.509(2)	C(24)	-	N(3)	1.141(2)
C(14)	-	C(15)	1.383(2)				

Table 46

Bond angles of the non-hydrogen atoms
with standard deviations in parentheses.

C(1)	-	C(2)	-	C(3)	115.0(2)
C(2)	-	C(3)	-	C(4)	113.3(2)
C(3)	-	C(4)	-	C(5)	114.8(2)
C(4)	-	C(5)	-	C(6)	113.6(2)
C(5)	-	C(6)	-	C(7)	113.6(2)
C(6)	-	C(7)	-	C(8)	115.3(1)
C(7)	-	C(8)	-	C(9)	112.5(1)
C(7)	-	C(8)	-	C(10)	111.5(1)
C(9)	-	C(8)	-	C(10)	109.9(2)
C(8)	-	C(9)	-	C(13)	112.7(1)
C(8)	-	C(10)	-	C(11)	113.2(1)
C(10)	-	C(11)	-	C(12)	111.4(1)
C(11)	-	C(12)	-	C(13)	109.5(2)
C(11)	-	C(12)	-	C(14)	112.2(1)
C(13)	-	C(12)	-	C(14)	113.4(1)
C(9)	-	C(13)	-	C(12)	112.0(1)
C(12)	-	C(14)	-	C(15)	124.6(2)
C(12)	-	C(14)	-	C(16)	121.3(1)
C(15)	-	C(14)	-	C(16)	114.1(2)
C(14)	-	C(15)	-	N(1)	123.9(2)
C(14)	-	C(16)	-	N(2)	124.1(2)
C(18)	-	C(17)	-	N(1)	117.0(1)
C(18)	-	C(17)	-	N(2)	117.5(2)
N(1)	-	C(17)	-	N(2)	125.6(2)
C(17)	-	C(18)	-	C(19)	120.6(2)
C(17)	-	C(18)	-	C(20)	120.6(1)
C(19)	-	C(18)	-	C(20)	118.8(2)
C(18)	-	C(19)	-	C(21)	120.9(2)
C(18)	-	C(20)	-	C(22)	120.6(2)
C(19)	-	C(21)	-	C(23)	119.8(2)
C(20)	-	C(22)	-	C(23)	119.9(2)
C(21)	-	C(23)	-	C(22)	120.0(2)
C(21)	-	C(23)	-	C(24)	118.9(1)
C(22)	-	C(23)	-	C(24)	121.1(2)
C(23)	-	C(24)	-	N(3)	178.7(2)
C(15)	-	N(1)	-	C(17)	116.2(1)
C(16)	-	N(2)	-	C(17)	116.1(2)

Table 4.7. Intermolecular contact distances less than 3.8 Å
(involving non-hydrogen atoms)

N1 - C3 ^a	3.766	N1 - C15 ^b	3.782
N2 - C18 ^c	3.573	N2 - C20 ^c	3.796
N3 - N3 ^d	3.494	N3 - C4 ^b	3.798
N3 - C9 ^a	3.657	N3 - C13 ^a	3.683
N3 - C22 ^d	3.494	N3 - C24 ^d	3.457
C16 - C1 ^e	3.769	C18 - C16 ^c	3.787
C20 - C16 ^c	3.743	C22 - C14 ^c	3.750
C22 - C16 ^c	3.726	C23 - C9 ^a	3.749
C23 - C16 ^c	3.753	C24 - C9 ^a	3.454
C24 - C24 ^d	3.782		

None: x, y, z a: $x-1, y, z$ b: $1-x, \bar{y}, \bar{z}$
c: $1-x, \bar{y}, 1-z$ d: $\bar{x}, \bar{y}, 1-z$ e: $-1+x, 1/2-y, 1/2+z$

observations^{2,3} and have expected values³⁸. The average C-C bond length in the alkyl chain (C₁-C₈) is 1.518(2) Å and is apparently influenced by thermal vibrations. For the same reason, the average bond angle in the alkyl chain is 114.03°. The cyano group bond length (C₂₄-N₃) is 1.141(2) Å, close to the value found in other mesogenic compounds^{39,40}.

The molecule as a whole is not planar; the phenyl ring, the pyrimidine ring and the heptyl chain are planar within 0.01, 0.01 and 0.06 Å respectively. The cyclohexyl ring is in the chair conformation. From the Newmann projection of Fig.4.2 it is seen that phenyl and pyrimidine rings make an angle of 15°. The coupling of the pyrimidine and cyclohexane rings is illustrated in Fig.4.2(a). The length of the molecule in the crystalline state is 23.5 Å, whereas its theoretical length is at a maximum 24 Å, indicating that the molecule is in its most extended conformation. Calculations with Sybil⁴¹ and Insight⁴² confirm this observation.

4.7.2. Molecular Packing

Figures 4.3 and 4.4 show the projections of the structure along [001] and [010] respectively. The molecules lie nearly extended in this phases, parallel to a-axis. In Fig.4.5, the projection of the structure along [100] has been shown; here the angle in the molecule is apparent. Molecules related by centre of symmetry are arranged in layers in ac plane and the layers are stacked along b-axis. The molecules in neighbouring layers are arranged in herring-bone like pattern. The transformation from the crystalline to the smectic is of reconstitutive⁴³ type rather than displacive. The intermolecular distances smaller than 3.8 Å are

given in Table 4.7. Most of these distances occur between the polar parts of the molecules, in particular between the molecules related through a centre of symmetry as observed from Figs. 4.3 and 4.4. These short contacts suggest associated pairs of molecules bound together by weak interactions between benzene rings, pyrimidine rings and cyano-groups, with the respective chains stretching out at both sides of the pair. The length of such a pair is approximately 28 \AA from the position of C_1 to and including C_1' . Taking into account a Van der Waals' radius for C_1 of 2 \AA , the total length of an associated pair is 32 \AA . From the X-ray diffraction photographs in smectic phase (chapter III) a layer thickness is found to be 33.7 \AA . This fact makes it plausible that layers in the smectic phase are built from pairs similar to those found in the present investigation. Discussions on solid-liquid crystalline phase transformation are given in the previous chapter.

We have successfully adopted the PC version of NRCVAX⁴⁴ crystal structure analysis software. The structure of HCCPP has been solved by using this package program also. Many of the calculations involved in structural analysis have been performed by using PC programs written by us.

References

1. S.Gupta, P.Mandal, S.Paul, M.D.Wit, K.Goubitz and H.schenk, Mol.Cryst.Liq.Cryst., 195, 149(1991).
2. P.Mandal, B.Majumdar, S.Paul, H.Schenk and K.Goubitz, Mol.Cryst.Liq.Cryst., 168, 135(1989).
3. P.Mandal, S.Paul, C.H.Stam and H.Schenk, Mol.Cryst.Liq.Cryst., 180B, 369(1990).
4. C.H.Stout and L.H.Jensen, X-ray Structure Determination, Macmillan Pub. Co. Inc, N.Y., page 195(1968).
5. M.J.Buerger, Crystal Structure Analysis, Wiley, N.Y., page 152(1960).
6. M.M.Woolfson, An Int. to X-ray crystallography Cambridge University Press, London, page 173(1970).
7. D.T.Cromer and J.T.Waber, Acta Cryst., 18, 194(1965).
8. R.F.Stewart, E.R.Davidson and W.T.Sympson, J.Chem.Phys., 42, 3175(1965).
9. H.Lipson and W.Cochran, The determination of crystal structures, G.Bell and Sons Ltd., London, pp.72, 301(1968).
10. A.J.C.Wilson, Nature, 150, 152(1942).
11. P.Debye, Ann.Phys.Lp., 46, 809(1915).
12. I.Karle and J.M.Stewart, Acta.Cryst., A32, 1005(1976).
13. D.Harker, and J.S.Kasper, Acta.Cryst., 3, 374(1948).
14. J.Karle and H.Humpton, Acta.Cryst., 3, 181(1950); Ibid, 9, 635(1956).
15. D.Sayre, Acta Cryst., 5, 60(1952).
16. W.Cochran, Acta Cryst., 5, 65(1952).
17. W.H.Zachariasen, Acta Cryst., 5, 68(1952).
18. W.Cochran, M.M.Woolfson, Acta Cryst., 8, 1(1955).

19. J.Karle and I.L.Karle, Acta Cryst., 21, 849(1966).
20. P.Main, S.E.Hull, L.Lessinger, G.Germain, J.P.Declercq and M.M.Woolfson, MULTAN-78, A system of computer program for the automatic solution of crystal structures for X-ray diffraction data (University of York, England and Louvain, Belgium, 1978).
21. G.M.Sheldrick, SHELX, Program for crystal structure determination. University of Cambridge, England, 1976.
- 22 C.T.Kiers and H.Schenk, SIMPEL B3, An automatic direct method program package, University of Amsterdam, 1983, H.Schenk, Recl. Trav. Chin. paysbas, 102, 1(1983).
23. S.R.Hall, J.M. Stewart and R.J.Munn, Acta Cryst., A36, 979(1980).
24. Yao Jia-Xing, Zheng Chao de, Qian Jin-Zi, Han Fu-Son, Gu Yuan-Xin and Fan Hai-Fu, "SAPI: A computer program for automatic solution of crystal structures from X-ray data", Institute of Physics, Academic Sinica, Beijing, China, 1985.
25. J.M.Stewart, The X-ray 76 System, Tech. Rep. TR-446, Computer Science Centre, University of Maryland, College Park, Maryland (1968).
26. Y.Jia-Xing, Acta Cryst., A37, 642(1981).
27. H.Hauptman and J.Karle, Solution of the phase problem 1, the centro symmetric crystal, A.C.A. Monography No. 3 (1953).
28. H.Schenk, Acta Cryst., A29, 77(1973a).
29. H.Schenk, Acta Cryst., A29, 480(1973b).
30. H.Schenk, J.G.H.de Jong, Acta Cryst., A29, 31(1973).
31. M.Simerska, Czech. J.Phys., 6, 1(1956).
32. G.Germain, P.Main and M.M.Woolfson, Acta Cryst., B26, 274(1970).

33. H.Schenk, Acta Cryst., B27, 2039(1971).
34. H.Schenk and C.T.Kiers, In methods and applications in crystallographic computing, eds. S.R.Hall and T.Ashida, Clarendon Press, Oxford, p. 96-105(1984).
35. A.R.Overbeek and H.Schenk, Proc.K.Ned.Akad.Wet., B79, 341(1976).
36. H.Schenk and J.G.H.de Jong, Acta Cryst., A29, 480(1973).
37. D.T.Cromer and J.B.Mann, Acta Cryst., A24, 321(1968).
38. International Tables for X-ray Crystallography, Vol.III, Kynoch Press, Birmingham (1962).
39. P.Mandal and S.Paul, Mol.Cryst.Liq.Cryst., 131, 223(1985).
40. P.Mandal, S.Paul, K.Goubitz and H.Schenk, Mol.Cryst.Liq.Cryst., 135, 35(1986).
41. Sybyl, Molecular Modeling Software, Ver. 5.2, Tripos Associates Inc., St. Louis, Missouri.
42. Insight, Molecular Modeling Software, Biosym Technol, Inc.
43. R.F.Bryan and P.G.Forcier, Mol.Cryst.Liq.Cryst., 60, 133 (1980).
44. PC version of The NRCVAX Crystal Structure System, P.S.White, Department of Chemistry, University of New Brunswick, Fredericton, New Brunswick, Canada, E3D 6E2.